ACS Photonics

Article

pubs.acs.org/journal/apchd5

# Isosbestic Thermoplasmonic Nanostructures

Khaled Metwally,[†] Serge Mensah,[†] and Guillaume Baffou*[,‡]

[†]LMA, Centrale Marseille, CNRS, UPR 7051, Aix Marseille Univ, F-13453, Marseille, France

[‡]Institut Fresnel, CNRS, Aix Marseille Univ, Centrale Marseille, Marseille, France

Supporting Information

**ABSTRACT:** This article introduces the concept of photothermal isosbesticity in plasmonics. In analogy with absorbance spectroscopy, this concept designates nanostructures that feature an invariance of their temperature increase upon varying the illumination polarization angle. We show that nontrivial (*i.e.*, noncentrosymmetric) isosbestic nanostructures exist and prove valuable when the optical near-field intensity remains, on the contrary, highly dependent on the illumination polarization. The concept is introduced with the case of a sphere-dimer, where the conditions for isosbesticity can be derived analytically. The cases of a spheroid and a disc-dimer are also studied in order to draw a general theory and explain how isosbesticity conditions can be obtained from the visible to the infrared range. Nontrivial isosbestic plasmonic nanostructures represent powerful systems to elucidate the origin (thermal or optical) of mechanisms involved in plasmonics-assisted nanochemistry, liquid−gas phase transition, or heat-assisted magnetic recording.

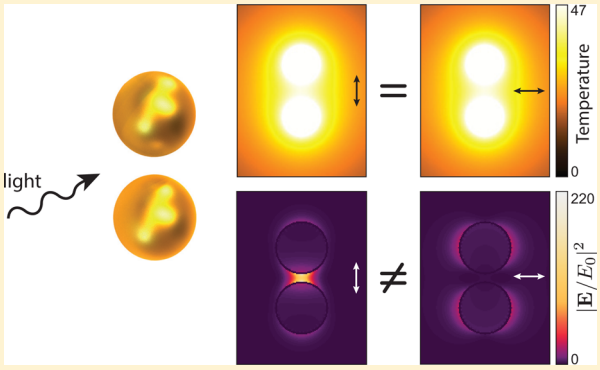


**KEYWORDS:** *plasmonics, nanoparticles, photothermal, thermoplasmonics*

Heat generation and near-field enhancement have been the main functionalities of metal nanoparticles for applications in nanoplasmonics. On the one hand, the gigantic optical near-field enhancements (NFEs) of metal nanotips or nanogaps prove valuable for applications in nanochemistry,[1] SERS, or heat-assisted magnetic recording (HAMR).[2−7] On the other hand, heat generation (HG) from gold nanoparticles is at the basis of numerous promising biomedical applications,[8] namely, photothermal cancer therapy,[9−12] drug and gene delivery,[13−16] or remote surgery.[17]

In this article, the concept of *photothermal isosbesticity* in nanoplasmonics is introduced. Isosbestic nanostructures are defined by an HG that is independent of the illumination polarization. The interest in isosbestic nanostructures becomes manifest when considering nanoparticles with no rotational invariance along the direction of light propagation (such as rods, dimers, spheroids, etc.), the near-field of which remains highly polarization dependent. The illustrative textbook case of a plasmonic sphere-dimer is treated in the first part, which is intended to give a physical picture of the concept with an analytical description of the dimer as interacting dipoles. Then, the case of a spheroid is also treated in order to propose a unified description of isosbesticity in plasmonics. These results are also aimed at giving the recipe for adjusting the isosbestic wavelength at will, from the visible range to the infrared. The final part of the article is devoted to explain how isosbestic structures can help identify the mechanisms (NFE or HG) in various plasmonics applications.

## DEFINITION OF PHOTOTHERMAL ISOSBESTICITY

Let us consider an optical plane wave traveling in a dielectric medium of refractive index $n_s$ ($n_s$ = 1.33 in this work) and characterized by a wave vector $\mathbf{k}$. An orthonormal frame (O, $x$, $y$, $z$) is oriented so that $\mathbf{k}$ is aligned with the (Oz) axis: $\mathbf{k} = \frac{2\pi n_s}{\lambda_0}\mathbf{u}_z$. In this case, the complex amplitude $\underline{\mathbf{E}}_0$ of the electric field of an incoming linearly polarized light reads $\underline{\mathbf{E}}_0(\mathbf{r})e^{-i\omega t} = E_0(\cos\theta\mathbf{u}_x + \sin\theta\mathbf{u}_y)e^{i\mathbf{k}\cdot\mathbf{r}-i\omega t}$ where $\omega = k/n_s c$ and $\theta$ defines the light polarization. In this article, all complex number quantities are underlined (such as $\underline{\mathbf{E}}_0$). The irradiance (power per unit area) $I$ of this plane wave reads thus $I = n_s c\varepsilon_0 {E_0}^2/2$.

Let us consider now an absorbing nanostructure within this medium, characterized by an absorption cross section $\sigma_{abs}$ such that the power absorbed by the nanostructure reads $P = \sigma_{abs}I$. In this work, an absorbing structure is said to be *isosbestic* relative to the wave vector $\mathbf{k}$ if its absorption cross section is independent of $\theta$. This adjective is borrowed from the field of molecular absorbance spectroscopy, where an isosbestic point refers to the wavelength for which the absorbance of a sample under chemical transformation is independent of a parameter, usually time (because reactants and products have the same molar absorptivity). Here, polarization rather than time is the parameter of interest, acting on the absorbance of the system. In a good approximation, the direct consequence of an invariance

**Received:** March 30, 2017
**Published:** May 30, 2017




DOI: 10.1021/acsphotonics.7b00329
*ACS Photonics* 2017, 4, 1544−1551

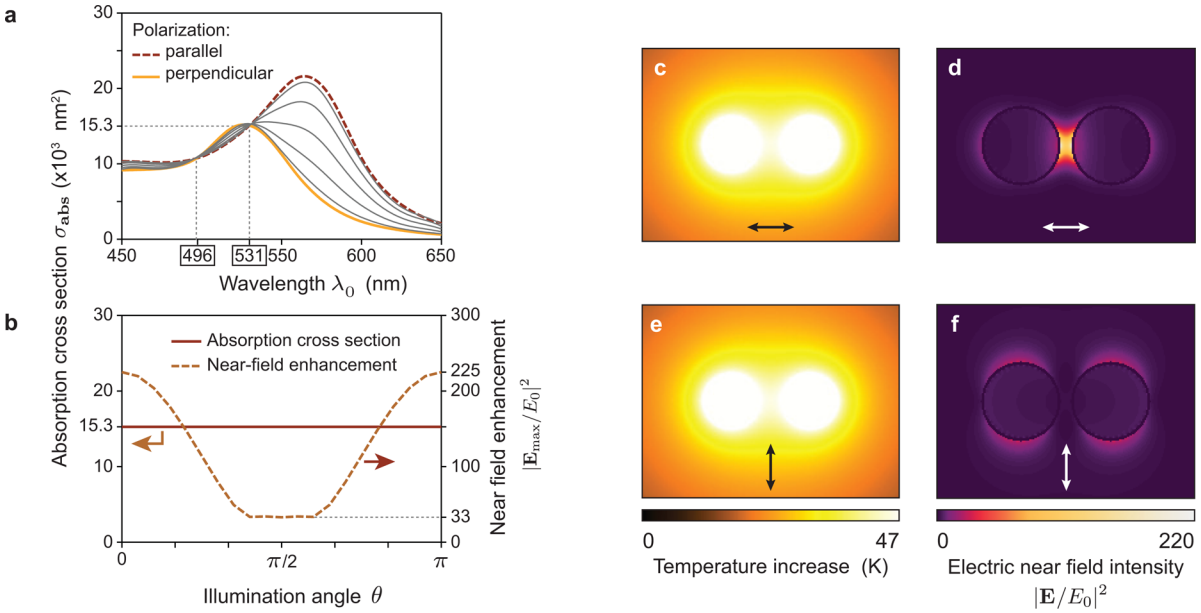


**Figure 1.** (a) Absorption cross section of a dimer structure composed of two 60 nm gold spheres in water separated by a 10 nm gap, for longitudinal and perpendicular polarizations of the incident light. Gray lines correspond to intermediate polarization angles (15°, 30°, 45°, 60°, and 75°). A crossing is observed for the isosbestic wavelengths $\lambda$ = 496 and 531 nm. (b) Absorption cross section and normalized electric near-field as functions of the illumination angle, at the isosbestic wavelength $\lambda$ = 531 nm, identified in (a). (c) Temperature map for a longitudinal polarization of the incident light and an arbitrary light irradiance of 1 mW/$\mu$m$^2$. (d) Corresponding normalized electric near-field. (e, f) Same as (c) and (d) for a perpendicular incident light polarization.

of the absorption cross section is an invariance of the temperature increase as well. A sphere is obviously isosbestic for any wave vector due to its point symmetry, but this case is not of particular interest. The response of any system endowed with a 3-fold symmetry (e.g., equilateral triangle) is also polarization-independent by nature. We coin these systems *trivial* isosbestic structures. Nontrivial isosbestic systems, which rather consist of nanoparticles that have no axial symmetry along the direction of light propagation (like rods or dimers), are much more relevant for several applications (as explained in the last section of this article).

## THE CASE OF A SPHERE DIMER

As an introductory nontrivial isosbestic structure, a dimer consisting of two neighboring nanospheres is considered herein. This example is ideal to introduce the concept of isosbesticity because it can be treated analytically in the dipolar approximation and it easily gives a physical picture of the underlying physics of isosbesticity in plasmonics. In this section, the sphere-dimer will be composed of two spheres aligned along the $(Ox)$ axis, in positions $\mathbf{r}_1 = (0, 0, 0)$ and $\mathbf{r}_2 = (d, 0, 0)$. They have a radius $a$, they are separated by a gap $g$, and their center-to-center distance is $d = |\mathbf{r}_1 - \mathbf{r}_2| = 2a + g$.

**Numerical Simulations.** Prior to presenting the analytical formalism, Figure 1 plots the results of numerical simulations for a sphere-dimer, in order to illustrate the concept. In this whole study, optical simulations have been conducted using the boundary element method (BEM)[18,19] and thermal simulations using a Green's function approach,[20] considering a water thermal conductivity of 0.6 W·m$^{-1}$·K$^{-1}$. The thermal conductivity of the nanoparticles was considered as infinite, which naturally results in uniform temperature distributions within the nanoparticles. This assumption is justified by the much larger thermal conductivity of gold compared to water (500 times larger). This assumption is usually valid in nanoplasmonics, no matter the size of the nanoparticles, provided the nanoparticles are not partially illuminated as shown in ref 21. Figure 1a plots the absorption cross section of a sphere-dimer structure in the case $a$ = 30 nm and $g$ = 10 nm, for perpendicular and parallel polarizations. An invariance of the absorption cross section is observed for $\lambda_0$ = 531 nm. This is the isosbestic wavelength according to the above-mentioned definition. The fact that all the cross section line shapes at different angles meet in a single point for some wavelength is not surprising. Any incoming linearly polarized light can be decomposed into two light beams crossed-polarized along the two main axes of the structure. So if the absorption cross sections for the transverse and longitudinal modes are equal, the absorption cross section naturally does not vary by changing the polarization angle. In other words, it suffices to find crossing points of the transverse and longitudinal spectra to make sure that the response of the structure is polarization-angle invariant. Note that this result illustrates a simple procedure to determine the isosbestic wavelength(s) of a plasmonic structure experimentally or numerically: It suffices to measure or compute the absorption cross section spectra of a given structure for the two orthogonal polarizations and to look for possible crossing points. At this isosbestic wavelength of 531 nm, the evolution of the absorption cross section and of the maximum NFE as a function of the illumination angle $\theta$ have been plotted in Figure 1b. This figure evidences that for this specific wavelength the energy absorption (and thus the temperature increase) is not dependent on the incident light polarization, while the NFE is highly polarization-dependent. The distributions of the temperature increase and near-field intensity for the two orthogonal polarizations are represented in Figure 1c,d. While the temperature maps remain identical, the optical near-field distributions are different in amplitude and shape.

Let us give some explanation about the physical origin of isosbesticity in the case of a sphere-dimer. The near-field



DOI: 10.1021/acsphotonics.7b00329
ACS Photonics 2017, 4, 1544−1551

enhancement of a dimer is bound to be highly polarization-dependent, no matter the wavelength, because of the presence of a gap. Within a gap, because of the proximity of the accumulated charges on both sides of the gap, the electric field is necessarily gigantic when the polarization is along the dimer axis, even out of resonance, which naturally implies a strong polarization dependence of the NFE. However, since the heat generation has nothing to do with the electric field within the gap, but rather with the electric field inside the metal, the presence of a gap does not prevent having a constant heat generation as a function of the light polarization, which opens the path for isosbesticity.

**Analytical Formalism in the Dipolar Approximation.** Determining the optical response of a dimer of nanospheres considered as two interacting dipoles is a self-consistent problem, governed by this set of equations:

$$\begin{cases} \underline{\mathbf{E}}_1^{\text{ext}} = \mathbf{E}_0(\mathbf{r}_1) + \underline{\mathbb{S}}_\omega(\mathbf{r}_1, \mathbf{r}_2)\underline{\alpha}\underline{\mathbf{E}}_2^{\text{ext}} \\ \underline{\mathbf{E}}_2^{\text{ext}} = \mathbf{E}_0(\mathbf{r}_2) + \underline{\mathbb{S}}_\omega(\mathbf{r}_2, \mathbf{r}_1)\underline{\alpha}\underline{\mathbf{E}}_1^{\text{ext}} \end{cases} \tag{1}$$

where $\underline{\mathbf{E}}_j^{\text{ext}}$ is the electric field experienced by sphere $j \in \{1, 2\}$, generated by its environment. It has two origins, the incoming plane wave $\underline{\mathbf{E}}_0$ and the electric field generated by the neighboring nanoparticle. $\underline{\alpha}\underline{\mathbf{E}}_j^{\text{ext}} = \underline{\mathbf{p}}_j$ is the polarization vector of sphere $j$ where $\underline{\alpha}$ is the complex polarizability of the sphere. $\underline{\mathbb{S}}_\omega(\mathbf{r}_m, \mathbf{r}_n)$ is the field propagator; it has a closed-form expression in a uniform medium given in the general case by[22]

$$\underline{\mathbb{S}}(\mathbf{r}_m, \mathbf{r}_n) = (-k^2\mathbb{I}_1(\mathbf{R}) - \mathrm{i}k\mathbb{I}_2(\mathbf{R}) + \mathbb{I}_3(\mathbf{R}))\frac{\mathrm{e}^{\mathrm{i}k|\mathbf{R}|}}{4\pi\varepsilon_0}$$

where

$$\mathbf{R} = \mathbf{r}_m - \mathbf{r}_n$$

$$\mathbb{I}_1(\mathbf{R}) = \frac{\mathbf{R}\cdot\mathbf{R}^{\mathrm{T}} - R^2\mathbb{I}}{R^3}$$

$$\mathbb{I}_2(\mathbf{R}) = \frac{3\mathbf{R}\cdot\mathbf{R}^{\mathrm{T}} - R^2\mathbb{I}}{R^4}$$

$$\mathbb{I}_3(\mathbf{R}) = \frac{3\mathbf{R}\cdot\mathbf{R}^{\mathrm{T}} - R^2\mathbb{I}}{R^5}$$

In this series of equations, $\mathbf{R}^{\mathrm{T}}$ means the transpose of the column vector $\mathbf{R}$, $R$ is the norm of $\mathbf{R}$, $\mathbb{I}$ is the identity matrix, $\mathbb{I}_1(\mathbf{R})$ represents the propagative field, while $\mathbb{I}_2(\mathbf{R})$ and $\mathbb{I}_3(\mathbf{R})$ represent the optical near-field. In the following, $\mathbb{I}_1$ will be neglected, although closed-form expressions of a dimer response can also be obtained without this approximation.[23] This approximation is valid if $kd \ll 1$. $\underline{\mathbb{S}}(\mathbf{r}_m, \mathbf{r}_n)$ is dependent only on the column vector $\mathbf{R}$ and is invariant by the inversion of $m$ and $n$. Thanks to these relations, system (1) can be recast into a self-consistent matrix equation involving only the unknowns $\underline{\mathbf{E}}_j^{\text{ext}}$. This system can be simplified. First, as the two nanoparticles are located in the $(Oxy)$ plane, the $z$ coordinate can be skipped and the dimension of the matrix equation reduced accordingly. Second, because of the symmetry of the sphere-dimer and of the illumination, the electric field experienced by each sphere must be identical: $\underline{\mathbf{E}}_1^{\text{ext}} = \underline{\mathbf{E}}_2^{\text{ext}} \triangleq \underline{\mathbf{E}}^{\text{ext}}$, as well as $\underline{\mathbf{E}}_0(\mathbf{r}_1) = \underline{\mathbf{E}}_0(\mathbf{r}_2) \triangleq \mathbf{E}_0$, which becomes a real vector. Thus, system (1) can be recast into a single equation with a single unknown, $\underline{\mathbf{E}}^{\text{ext}} = \underline{E}_x^{\text{ext}}\mathbf{u}_x + \underline{E}_y^{\text{ext}}\mathbf{u}_y$:

$$\underline{\mathbf{E}}^{\text{ext}} = \mathbf{E}_0 + \underline{\mathbb{S}}(\mathbf{r}_1, \mathbf{r}_2)\underline{\alpha}\underline{\mathbf{E}}^{\text{ext}} \tag{2}$$

$$\underline{\mathbf{E}}^{\text{ext}} = [1 - \underline{\alpha}\underline{\mathbb{S}}(\mathbf{r}_1, \mathbf{r}_2)]^{-1}\mathbf{E}_0 \tag{3}$$

$$\begin{pmatrix} \underline{E}_x^{\text{ext}} \\ \underline{E}_y^{\text{ext}} \end{pmatrix} = \begin{pmatrix} 1 - 2\underline{s} & 0 \\ 0 & 1 + \underline{s} \end{pmatrix}^{-1} \cdot \begin{pmatrix} E_0\cos\theta \\ E_0\sin\theta \end{pmatrix} \tag{4}$$

where

$$\underline{s} \triangleq \underline{\alpha}\frac{1 - \mathrm{i}kd}{4\pi\varepsilon_0 d^3}\mathrm{e}^{\mathrm{i}kd} \tag{5}$$

Hence, calculating $\underline{\mathbf{E}}^{\text{ext}}$ just implies the inversion of a simple $2 \times 2$ diagonal matrix. It finally yields

$$\underline{E}_x^{\text{ext}} = E_0\frac{\cos\theta}{1 - 2\underline{s}}, \underline{E}_y^{\text{ext}} = E_0\frac{\sin\theta}{1 + \underline{s}} \tag{6}$$

The condition of isosbesticity reads "$|\underline{\mathbf{E}}^{\text{ext}}|^2$ independent of $\theta$" where

$$|\underline{\mathbf{E}}^{\text{ext}}|^2 = \left|\frac{E_0\cos\theta}{1 - 2\underline{s}}\right|^2 + \left|\frac{E_0\sin\theta}{1 + \underline{s}}\right|^2 \tag{7}$$

This implies $|1 - 2\underline{s}| = |1 + \underline{s}|$, or equivalently

$$|\underline{s} - 1| = 1 \tag{8}$$

The expression of $\underline{s}$ can be expressed from eq 5 by calculating $\underline{\alpha}$ using the following closed-form expression, valid for small values of $ka$:[24]

$$\underline{\alpha} = \varepsilon_0\varepsilon_s V\frac{1 - \left(\frac{1}{10}\right)(\underline{\varepsilon} + \varepsilon_s)x^2}{\left(\frac{1}{3} + \frac{\varepsilon_s}{\underline{\varepsilon} - \varepsilon_s}\right) - \frac{1}{30}(\underline{\varepsilon} + 10\varepsilon_s)x^2 - \mathrm{i}\frac{16}{9}\varepsilon_s^{3/2}x^3} \tag{9}$$

where $\varepsilon_s = n_s^2$, $\underline{\varepsilon}$ is the permittivity of the nanoparticle material (taken from Johnson and Christy's[25] data set in our simulations using gold), $V = \frac{4\pi}{3}a^3$, and $x = \frac{\pi a}{\lambda_0}$. Refined estimations of $\underline{\alpha}$ can be obtained numerically using the Mie theory of higher orders.[26]

Hence, writing $\underline{s} = s' + \mathrm{i}s''$, the condition of isosbesticity considered in the $(s', s'')$ complex plane is elegantly described by a circle of radius 1 centered in $(s', s'') = (1, 0)$. The derivation of this condition is provided in the SI (as a Mathematica notebook). This condition has to be compared with the actual expression of $\underline{s}$, which can be expressed from eq 5 using, for instance, a closed-form expression of $\underline{\alpha}$[24] or Mie theory.[26]

In Figure 2, representing the $(s', s'')$ complex plane, the condition of isosbesticity (eq 8) corresponds to a circle represented by a solid line, and the actual values of $\underline{s}$ defined by eq 5 are represented by dashed lines, for three different dimer geometries. The isosbestic conditions correspond to crossings of these two lines. In the case $a = 30$ nm and $g = 10$ nm, an isosbestic condition is fulfilled at $\lambda_0 = 527$ nm. Noteworthily, this is in good agreement with the numerical simulations reproduced in Figure 1 for the same morphology that predicted an isosbestic wavelength of 531 nm.

Making the spheres bigger and reducing the gap make the isosbestic wavelength larger, up to 550 nm in the case of $a = 40$ nm and $g = 5$ nm. The effect of enlarging an asymmetric structure (no rotational invariance along the direction of propagation) such as a sphere-dimer is to damp the stronger (longitudinal) resonance with respect to the weaker (transverse). As a consequence, the two spectra get closer, which increases the chance to observe crossing points. However, for smaller spheres and/or larger gaps, no isosbesticity condition occurs, as in the



DOI: 10.1021/acsphotonics.7b00329
ACS Photonics 2017, 4, 1544−1551

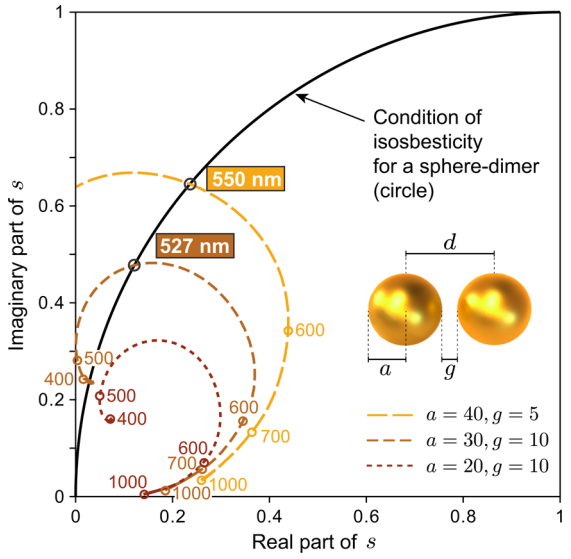


**Figure 2.** Space of $\underline{s}$ values for a gold sphere-dimer in water in the complex space. The black solid line represents the values that $\underline{s}$ must equal to obtain an isosbestic sphere-dimer. Dashed lines represent the actual values of $\underline{s}$ as a function of the wavelength from $\lambda = 400$ to $\lambda = 1000$ nm, for three different gold sphere-dimer morphologies $(a, g)$. Particular wavelength values have been indicated, in particular the isosbestic wavelength (boxed numbers).

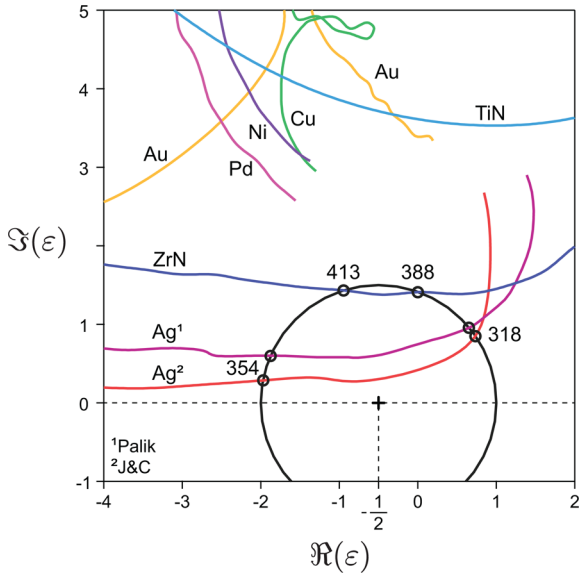


**Figure 3.** Polar plots of the complex permittivity of common plasmonic materials. The condition given by eq 11 is represented as a solid line circle. Only materials crossing this circle can exhibit isosbestic conditions in the quasistatic regime.

case of $a = 20$ nm and $g = 10$ nm. Thus, the existence of an isosbestic wavelength for a given nanoparticle geometry *is not systematic*.

**Isosbesticity with Materials Other than Gold.** As shown above, for gold, no solution of eq 8 exists for small enough nanoparticles, i.e., for small values of $|\underline{s}|$ ($\lim_{a\to 0}\underline{s} = 0$). One could wonder why and one could wonder if this happens for any material. Equation 8 can be fulfilled at the first order for arbitrarily small values of $\underline{s}$ if $\underline{s}$ is an imaginary number. For small nanoparticles, one can consider a first-order approximation of $\underline{s}$ using eqs 5 and 9, which yields

$$\underline{s} = \varepsilon_s \frac{a^3}{d^3} \frac{\underline{\varepsilon} - \varepsilon_s}{\underline{\varepsilon} + 2\varepsilon_s} \tag{10}$$

Consequently, eq 8 can be fulfilled for arbitrarily small nanoparticles only if the permittivity of the material can fulfill

$$\Re\left(\frac{\underline{\varepsilon} - \varepsilon_s}{\underline{\varepsilon} + 2\varepsilon_s}\right) = 0 \tag{11}$$

or equivalently $|\underline{\varepsilon}|^2 + \varepsilon' = 2$, or equivalently

$$\left(\varepsilon' + \frac{1}{2}\right)^2 + (\varepsilon'')^2 = \left(\frac{3}{2}\right)^2 \tag{12}$$

which is the equation of a circle in the complex plane of $\underline{\varepsilon}$.

This condition never happens for gold irrespectively of the wavelength. It is actually even very rare in plasmonics. According to our investigations, it only occurs for silver (Ag) and zirconium nitride (ZrN). Interestingly, this result makes Ag and ZrN singular materials in plasmonics. Figure 3 displays polar plots of the complex permittivity of several metals used in plasmonics, along with the circle corresponding to eq 12. The materials we have considered are Ag, Al, Au, Co, Cr, Cu, Fe, Mn, Mo, Ni, Pd, Pt, Ta, TiN, and ZrN, and we have only plotted the permittivity values down to $\lambda = 300$ nm. Other materials can exhibit isosbestic points such as Hg or Al, but at very low wavelengths close to 100 nm. They have not been represented in Figure 3.

These results are corroborated by numerical simulations presented in Figure 4a–f. Both small and large nanoparticles composed of Au, ZrN, and Ag have been modeled. While a small sphere-dimer made of gold does not exhibit isosbestic points (Figure 4a), small sphere-dimers made of ZrN and Ag feature isosbestic conditions for specific wavelengths (Figure 4b,c). For larger structures, isosbestic conditions can be obtained for any material (Figure 4d–f).

## THE CASE OF SPHEROIDS

Spheroids represent another textbook case that deserves attention. For small spheroids in the quasistatic regime, the condition of isosbesticity can be derived analytically as well. Using Mie–Gans theory[27] and the expression of the Joule number defined in ref 28, the isosbestic condition reads

$$|1 - 3L_1\xi_1| = |1 - 3L_3\xi_3| \tag{13}$$

where

$$\xi_j = \frac{1}{3}\frac{\varepsilon - \varepsilon_s}{\varepsilon_s + L_j(\varepsilon - \varepsilon_s)} \tag{14}$$

and where $L_j$ are the depolarization factors. For a sphere $L_x = L_z = 1/3$. For a prolate spheroid along the $z$ direction, $L_z < L_x$, but $2L_x + L_z = 1/3$ remains constant. Replacing $\xi_j$ in eq 13 by its expression in 14, one gets

$$\left|1 - \frac{L_x(\varepsilon - \varepsilon_s)}{\varepsilon_s + L_x(\varepsilon - \varepsilon_s)}\right| = \left|1 - \frac{L_z(\varepsilon - \varepsilon_s)}{\varepsilon_s + L_z(\varepsilon - \varepsilon_s)}\right| \tag{15}$$

$$\left|\frac{\varepsilon_s}{\varepsilon_s + L_x(\varepsilon - \varepsilon_s)}\right| = \left|\frac{\varepsilon_s}{\varepsilon_s + L_z(\varepsilon - \varepsilon_s)}\right| \tag{16}$$

$$|\varepsilon_s + L_x(\varepsilon - \varepsilon_s)| = |\varepsilon_s + L_z(\varepsilon - \varepsilon_s)| \tag{17}$$



DOI: 10.1021/acsphotonics.7b00329
ACS Photonics 2017, 4, 1544–1551

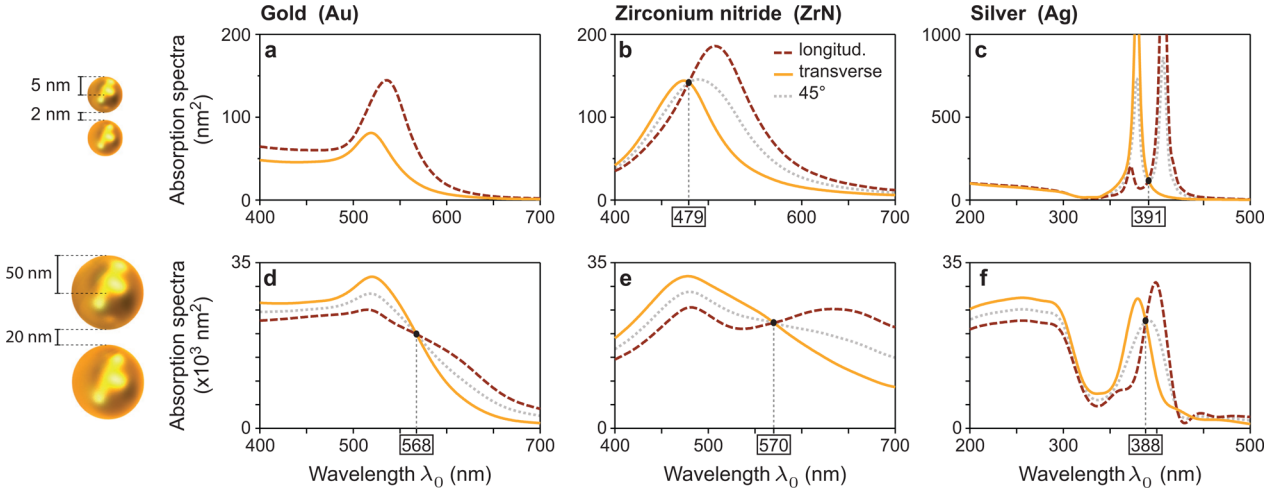


**Figure 4.** Calculations of cross-polarization absorption spectra using the BEM for different spheroid sizes and materials. (a−c) Small sphere-dimer composed of two 20 nm spheres separated by a gap of 2 nm. (d−f) Large sphere-dimer composed of two 200 nm spheres separated by a gap of 20 nm. (a, d) Case of Au. (b, e) Case of ZrN. (c, f) Case of Ag. Dashed lines correspond to calculations with light polarization parallel to the axis of the dimer. Solid lines correspond to light polarization perpendicular to the dimer axis. Dotted lines correspond to an intermediate light polarization (45°).

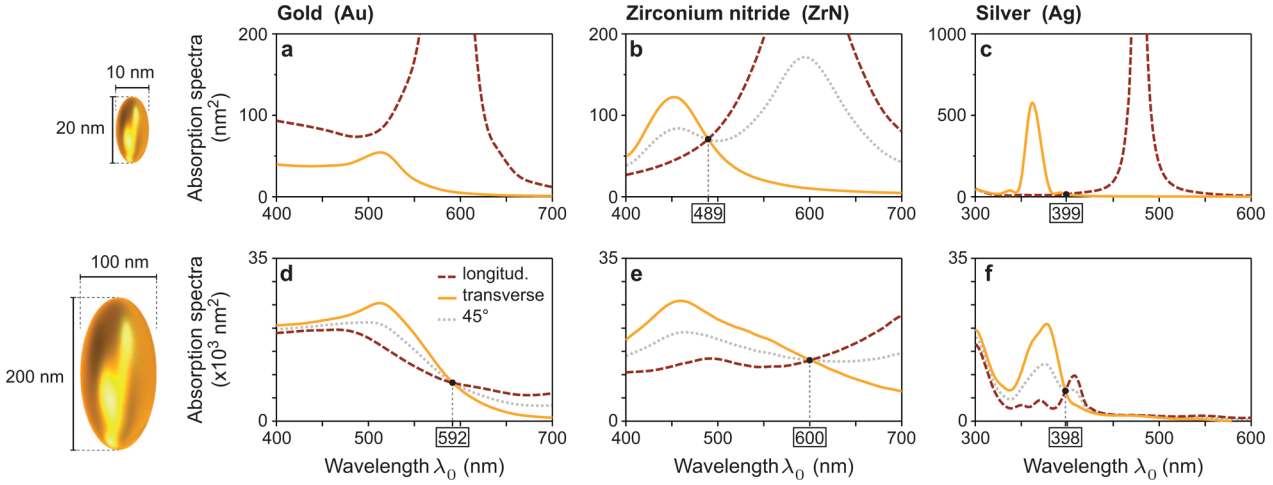


**Figure 5.** Calculations of cross-polarization absorption spectra using the BEM for different spheroid sizes and materials. (a−c) Small prolate spheroids of 10 nm × 20 nm. (d−f) Large prolate spheroids of 100 nm × 200 nm. (a, d) Case of Au. (b, e) Case of ZrN. (c, f) Case of Ag. Dashed lines correspond to calculations with a light polarization parallel to the long axis of the spheroid. Solid lines correspond to a light polarization along the short axis of the spheroid. Dotted lines correspond to an intermediate light polarization (45°).

Let us now consider a small elongation from a sphere along the $z$ axis. In this case, one has

$$L_x = \frac{1}{3} + \delta L \tag{18}$$

$$L_z = \frac{1}{3} - 2\delta L \tag{19}$$

where $\delta L$ is arbitrarily small. Equation 17 now gives

$$\left|\frac{2\varepsilon_s}{3} + \frac{\varepsilon}{3} + (\varepsilon - \varepsilon_s)\,\delta L\right| = \left|\frac{2\varepsilon_s}{3} + \frac{\varepsilon}{3} - 2(\varepsilon - \varepsilon_s)\,\delta L\right|$$

$$|1 + 3\xi\delta L| = |1 - 6\xi\delta L|$$

$$\left|\frac{1 + 3\xi\delta L}{1 - 6\xi\delta L}\right| = 1 \tag{20}$$

where

$$\xi = \frac{\varepsilon - \varepsilon_s}{\varepsilon + 2\varepsilon_s} \tag{21}$$

At the first order of $\delta L$, eq 20 gives

$$|(1 + 3\xi\delta L)(1 + 6\xi\delta L)| \approx 1$$

$$|1 + 9\xi\delta L| \approx 1 \tag{22}$$

Just like eq 8, this equation has a solution for $\delta L$ arbitrarily small if $\xi$ is imaginary, i.e., if

$$\Re(\xi) = \Re\left(\frac{\varepsilon - \varepsilon_s}{\varepsilon + 2\varepsilon_s}\right) = 0 \tag{23}$$

which is exactly the same condition as in the case of a sphere-dimer. Consequently, eq 23 seems to be a general condition to achieve isosbesticity in plasmonics for small nanoparticles. Since we could derive this condition only for dimers and elongated nanoparticles, this rule of thumb is only conjecture.



DOI: 10.1021/acsphotonics.7b00329
ACS Photonics 2017, 4, 1544−1551

These results are corroborated by numerical simulations presented in Figure 5a–f. Both small and large nanoparticles composed of Au, ZrN, and Ag have been modeled. While a small spheroid made of gold does not exhibit isosbestic points (Figure 5a), small spheroids made of ZrN and Ag feature isosbestic conditions for specific wavelengths (Figure 5b,c). For larger structures, isosbestic conditions can be obtained for any material (Figure 5d–f).

## HOW TO ADJUST THE ISOSBESTIC WAVELENGTH

Just like the case of a sphere-dimer again, the isosbesticity wavelength for a spheroid remains in the green region of the spectrum, close to the resonance wavelength of a dipolar gold sphere. For structures with 2-fold symmetries, the isosbestic wavelength is actually supposed to be close to the resonance wavelength corresponding to the transverse mode, i.e., when the polarization of the incoming light is along the shorter dimension of the structure. This is why sphere-dimers and spheroids are isosbestic around $\lambda$ = 530 nm. In order to shift the isosbestic wavelength to higher values, it suffices therefore to consider structures with a red-shifted transverse resonance. Structures made by e-beam lithography typically behave this way. We conducted numerical simulations of the cross-polarization spectra of disc-dimers of various thicknesses (see Figure 6). In each case, the discs are 60 nm in diameter and separated by a gap of 10 nm, but their thickness varies from 10 to 60 nm. Varying the thickness makes it possible to vary the transverse resonance. For a thickness of 60 nm, corresponding to the diameter of a disc, the resonance is close to that of a sphere and the isosbestic wavelength is 542 nm, close to the resonance of a sphere. For much smaller thicknesses, the transverse aspect ratio is increased, which naturally increases the transverse resonance wavelength and the isosbestic wavelength. Results of this section evidence that engineering the transverse resonance of plasmonic nanostructures enables the selection of isosbestic conditions over the entire visible–near-IR range using gold. Disc-dimers, which can be easily designed using e-beam lithography, appear to be efficient structures for this purpose.

The absorption spectra of a disc-dimer for longitudinal and transverse illuminations have been calculated using BEM (Figure 6). Both polarizations feature a red-shifted resonance, which naturally drives the isosbestic wavelengths to higher values. Thus, the isosbestic wavelength can be a priori adjusted at will, which is a strong benefit to address a wide range of applications.

## DISCUSSION

The influence of the light polarization on plasmonic structures and related invariances have been reported in the literature. First, the presence of isosbestic points in plasmonics were first mentioned by Thompson et al. in 2011,[29] but the definition was different. This work rather dealt with the transmission intensity through plasmonic arrays, not photothermal effects. Second, in 2016, Geraci et al. investigated invariances with plasmonic trimers.[30] The authors explained that the usual strong dependence of the optical response of plasmonic nanoparticles on the incident light polarization can be problematic for some applications. To address this problem, disc-trimer structures have been shown to be possible candidates. However, the authors focused on a different objective compared to our work: a broadband invariance of the optical response while we are seeking invariance of the heat generation while maintaining substantial dependence of the optical response. Finally, Lachaine

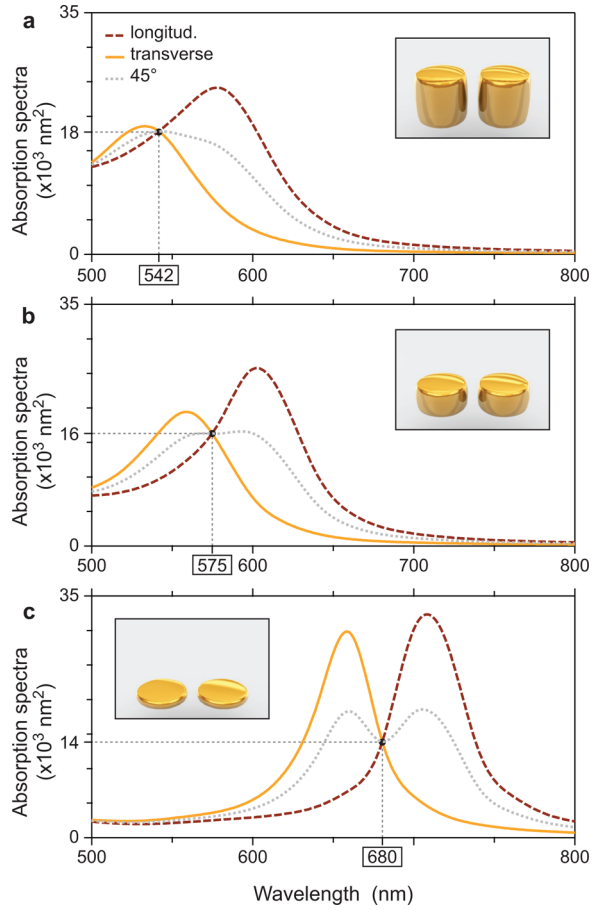


**Figure 6.** Calculations of cross-polarization absorption spectra using the BEM for different gold disc-dimer thicknesses $e$: (a) $e$ = 60 nm, (b) $e$ = 30 nm, and (c) $e$ = 10 nm. Insets represent the morphology of the structures. The illumination axis is vertical on these insets. Dashed lines correspond to calculations with light polarization parallel to the axis of the dimer. Solid lines correspond to light polarization perpendicular to the dimer axis. Dotted lines correspond to an intermediate light polarization (45°).

et al. evidenced an invariance of heat generation from gold spheres from linear to circular polarizations.[31]

Isosbesticity is a concept that can be beneficial for several applications in plasmonics. In nanochemistry, plasmonic nanostructures can favor chemical reactions.[1] However, the origin of this enhancement is not always straightforward. Both an NFE and an HG can be at the origin of an increase of the yield of a chemical reaction, and both these quantities are difficult to discriminate at the nanoscale in samples used in nanochemistry. In 2009, this problem was honestly pointed out by the group of El Sayed.[32] Very often, thermal effects are experimentally[33] or numerically[34] underestimated because of inappropriate approaches. A plasmonic structure behaving just like in Figure 1 could be used to straightforwardly discriminate one mechanism or another (HG or NFE), experimentally. If the chemical yield produced by nontrivial isosbestic nanostructures proves independent of incident light polarization, it will evidence a thermal-induced effect, while if it is strongly polarization-dependent, it will rather highlight a photochemical process. Other applications of plasmonics also suffer from this blurred duality, such as in HAMR:[2,3] in this application, the near-field intensity of a plasmonic nanoantenna localized a few nanometers away from a hard-disk drive is supposed to transfer energy via its


DOI: 10.1021/acsphotonics.7b00329
ACS Photonics 2017, 4, 1544–1551

optical near-field toward the disk to locally increase the disk temperature. However, a temperature increase due to *thermal* radiation (not optical radiation) is also possible, although it was never demonstrated. The use of isosbestic plasmonic structures could decipher between both transduction pathways: an optical near-field transfer or a thermal radiation near-field transfer. Finally, the origin of bubble generation around plasmonic nanoparticles under pulsed illumination is also unclear and suffers from the same dual issue: besides a simple heating mechanism, the generation of a plasma due to a strong electric near-field enhancement could also be responsible for bubble generation, especially under femtosecond pulsed illumination.[31,35] Generating a bubble around metal nanoparticles under pulsed illumination at the isosbestic wavelength of the nanoparticles (typically rods immobilized on a substrate) could confidently reveal the nature of the underlying mechanism of bubble formation.

Note that the concept of photothermal isosbesticity in plasmonics could be extended to the case of circular polarization and chiral nanostructures.[36−38] The optical properties of chiral plasmonic structures depend on the left- or right-handed nature of an incoming circular illumination. Thus, possible isosbesticity could be a priori obtained when observing crossing points in the absorption spectra corresponding to left- and right-handed polarization, i.e., for zero circular dichroism (CD), as defined in ref 36. This idea will possibly be further investigated in a future study.

In summary, we introduced the concept of isosbestic plasmonic structures in nanoplasmonics and give all the recipes to make an efficient use of it: (i) Isosbestic conditions are not always possible for a given nanoparticle morphology, (ii) Ag and ZrN are singular isosbestic materials, (iii) the isosbestic wavelength can be found for a given morphology by considering the intercrossing of two cross-polarized absorption spectra, (iv) enlarging nanoparticles favor the occurrence of isosbesticity, (v) the isosbestic wavelength can be arbitrarily chosen by engineering the transverse resonance wavelength of the nanoparticle. Finally, we have explained how such a class of plasmonic structures can have powerful applications for elucidating mechanisms in many applications such as nanochemistry, heat-assisted magnetic recording, or microbubble formation.

## ■ ASSOCIATED CONTENT

### Supporting Information

The Supporting Information is available free of charge on the ACS Publications website at DOI: 10.1021/acsphotonics.7b00329.

Additional information (ZIP)

## ■ AUTHOR INFORMATION


### Corresponding Author

*E-mail: guillaume.baffou@fresnel.fr.

### ORCID

Guillaume Baffou: 0000-0003-0488-1362


### Notes

The authors declare no competing financial interest.

## ■ ACKNOWLEDGMENTS

The authors wish to acknowledge financial support from ITMO Cancer AVIESAN (Alliance Nationale pour les Sciences de la Vie et de la Santé, National Alliance for Life Sciences & Health) within the framework of the Cancer Plan (GRAVITY project) and from the Agence National de la Recherche (PlasmoTherm project, ANR-15-CE24-0025-01).

## ■ REFERENCES


(1) Baffou, G.; Quidant, R. Nanoplasmonics for Chemistry. *Chem. Soc. Rev.* **2014**, *43*, 3898−3907.

(2) Stipe, B. C.; et al. Magnetic Recording at 1.5 Pb $m^{-2}$ Using an Integrated Plasmonic Antenna. *Nat. Photonics* **2010**, *4*, 484−488.

(3) Pan, L.; Bogy, D. B. Heat-Assisted Magnetic Recording. *Nat. Photonics* **2009**, *3*, 189−190.

(4) Challener, W. A.; Peng, C.; Itagi, A. V.; Karns, D.; Peng, W.; Peng, Y.; Yang, X. M.; Zhu, X.; Gokemeijer, N. J.; Hsia, Y.-T.; Ju, G.; Rottmayer, R. E.; Seigler, M. A.; Gage, E. C. Heat-Assisted Magnetic Recording by a Near-Field Transducer with Efficient Optical Energy Transfer. *Nat. Photonics* **2009**, *3*, 220−224.

(5) Kryder, M. H.; Gage, E. C.; McDaniel, T. W.; Challener, W. A.; Rottmayer, R. E.; Ju, G.; Hsia, Y.-T.; Erden, M. F. Heat Assisted Magnetic Recording. *Proc. IEEE* **2008**, *96*, 1810−1835.

(6) Zhang, Z.; Mayergoyz, I. D. The Use of Plasmonic Resonances in Thermally Assisted Magnetic Recording. *J. Appl. Phys.* **2008**, *103*, 07F510.

(7) Matsumoto, T.; Nakamura, K.; Nishida, T.; Hieda, H.; Kikitsu, A.; Naito, K.; Koda, T. Thermally Assisted Magnetic Recording on a Bit-Patterned Medium by Using a Near-Field Optical Head with a Beaked Metallic Plate. *Appl. Phys. Lett.* **2008**, *93*, 031108.

(8) Baffou, G.; Quidant, R. Thermo-plasmonics: Using Metallic Nanostructures as Nano-Sources of Heat. *Laser & Photon. Rev.* **2013**, *7*, 171−187.

(9) Jain, P. K.; El-Sayed, I. H.; El-Sayed, M. A. Au Nanoparticles Target Cancer. *Nano Today* **2007**, *2*, 18.

(10) Huang, X. H.; Jain, P. K.; El-Sayed, I. H.; El-Sayed, M. A. Gold Nanoparticles: Interesting Optical Properties and Recent Applications in Cancer Diagnostic and Therapy. *Nanomedicine* **2007**, *2*, 681−693.

(11) Gobin, A. M.; Lee, M. H.; Halas, N. J.; James, W. D.; Drezek, R. A.; West, J. L. Near-Infrared Resonant Nanoshells for Combined Optical Imaging and Photothermal Cancer Therapy. *Nano Lett.* **2007**, *7*, 1929−1934.

(12) Gu, F. X.; Karnik, R.; Wang, A. Z.; Alexis, F.; Levy-Nissenbaum, E.; Hong, S.; Langer, R. S.; Farokhzad, O. C. Targeted Nanoparticles for Cancer Therapy. *Nano Today* **2007**, *2*, 14.

(13) Doane, T. L.; Burda, C. The Unique Role of Nanoparticles in Nanomedicine: Imaging, Drug Delivery and Therapy. *Chem. Soc. Rev.* **2012**, *41*, 2885−2911.

(14) Lévy, R.; Shaheen, U.; Cesbron, Y.; Sée, V. Gold Nanoparticles Delivery in Mammalian Live Cells: a Critical Review. *Nano Rev.* **2010**, *1*, 4889.

(15) Ghosh, P.; Han, G.; De, M.; Kim, C. K.; Rotello, V. M. Gold Nanoparticles in Delivery Applications. *Adv. Drug Delivery Rev.* **2008**, *60*, 1307−1315.

(16) Han, G.; Ghosh, P.; De, M.; Rotello, V. M. Drug and Gene Delivery Using Gold Nanoparticles. *NanoBiotechnology* **2007**, *3*, 40.

(17) Kharlamov, A. N.; Tyurnina, A. E.; Veselova, V. S.; Kovtun, O. P.; Shur, V. Y.; Gabinsky, J. L. Silica-gold Nanoparticles for Atheroprotective Management of Plaques: Results of the NANOM-FIM Trial. *Nanoscale* **2015**, *7*, 8003−8015.

(18) Hohenester, U.; Trügler, A. MNPBEM - A Matlab Toolbox For the Simulation of Plasmonic Nanoparticles. *Comput. Phys. Commun.* **2012**, *183*, 370−381.

(19) García de Abajo, F. J.; Howie, A. Retarded Field Calculation of Electron Energy Loss in Inhomogeneous Dielectrics. *Phys. Rev. B: Condens. Matter Mater. Phys.* **2002**, *65*, 115418.

(20) Baffou, G.; Quidant, R.; Girard, C. Thermoplasmonics Modeling: a Green's Function Approach. *Phys. Rev. B: Condens. Matter Mater. Phys.* **2010**, *82*, 165424.

(21) Baffou, G.; Quidant, R.; García de Abajo, F. J. Nanoscale Control of Optical Heating in Complex Plasmonic Systems. *ACS Nano* **2010**, *4*, 709.




DOI: 10.1021/acsphotonics.7b00329
*ACS Photonics* 2017, 4, 1544−1551

(22) Baffou, G. Luminescence induite par microscopie à effet tunnel et étude des propriétés électroniques, chimiques et optiques de la surface de carbure de silicium 6H-SiC(0001)3 × 3. Ph.D. thesis, Université Paris XI, 2007.
(23) Rolly, B.; Stout, B.; Bonod, N. Metallic Dimers: When Bonding Transverse modes Shine Light. *Phys. Rev. B: Condens. Matter Mater. Phys.* **2011**, *84*, 125420.
(24) Maier, S. A. *Plasmonics, Fundamentals and Applications*; Springer, 2007.
(25) Johnson, P. B.; Christy, R. W. Optical Constants of the Noble Metals. *Phys. Rev. B* **1972**, *6*, 4370.
(26) Metwally, K.; Mensah, S.; Baffou, G. Fluence Threshold for Photothermal Bubble Generation Using Plasmonic Nanoparticles. *J. Phys. Chem. C* **2015**, *119*, 28586−28596.
(27) Myroshnychenko, V.; Rodríguez-Fernández, J.; Pastoriza-Santos, I.; Funston, A. M.; Novo, C.; Mulvaney, P.; Liz-Marzán, L. M.; García de Abajo, F. J. Modeling the optical response of gold nanoparticles. *Chem. Soc. Rev.* **2008**, *37*, 1792−1805.
(28) Lalisse, A.; Tessier, G.; Plain, J.; Baffou, G. Quantifying the Efficiency of Plasmonic Materials for Near-Field Enhancement and Photothermal Conversion. *J. Phys. Chem. C* **2015**, *119*, 25518−25528.
(29) Thompson, P. G.; Biris, C. G.; Osley, E. J.; Gaathon, O.; Osgood, R. M.; Panoiu, N. C.; Warburton, P. A. Polarization-Induced Tunability of Localized Surface Plasmon Resonances in Arrays of sub-Wavelength Cruciform Apertures. *Opt. Express* **2011**, *19*, 25035−25047.
(30) Geraci, G.; Hopkins, B.; Miroshnichenko, A. E.; Erkihun, B.; Neshev, D.; Kivshar, Y. S.; Maier, S. A.; Rahmani, M. Polarisation-Independent Enhanced Scattering by Tailoring Asymmetric Plasmonic Systems. *Nanoscale* **2016**, *8*, 6021−6027.
(31) Lachaine, R.; Boulais, E.; Meunier, M. From Thermo- to Plasma-Mediated Ultrafast Laser-Induced Plasmonic Nanobubbles. *ACS Photonics* **2014**, *1*, 331−336.
(32) Yen, C. W.; El-Sayed, M. A. Plasmonic Field Effect on the Hexacyanoferrate (III)-Thiosulfate Electron Transfer Catalytic Reaction on Gold Nanoparticles: Electromagnetic or Thermal? *J. Phys. Chem. C* **2009**, *113*, 19585−19590.
(33) Christopher, P.; Xin, H.; Linic, S. Visible-Light-Enhanced Catalytic Oxidation Reactions on Plasmonic Silver Nanostructures. *Nat. Chem.* **2011**, *3*, 467−472.
(34) Neumann, O.; Urban, A. S.; Day, J.; Lal, S.; Nordlander, P.; Halas, N. J. Solar Vapor Generation enabled by nanoparticles. *ACS Nano* **2013**, *7*, 42−49.
(35) Boulais, E.; Lachaine, R.; Meunier, M. Plasma Mediated off-Resonance Plasmonic Enhanced Ultrafast Laser-Induced Nanocavitation. *Nano Lett.* **2012**, *12*, 4763−4769.
(36) Fan, Z.; Govorov, A. O. Chiral Nanocrystals: Plasmonic Spectra and Circular Dichroism. *Nano Lett.* **2012**, *21*, 3283−3289.
(37) Valev, V. K.; Baumberg, J. J.; Sibilia, C.; Verbiest, T. Chirality and Chiroptical Effects in Plasmonic Nanostructures: Fundamentals, Recent Progress, and Outlook. *Adv. Mater.* **2013**, *25*, 2517−2534.
(38) Schäferling, M. *Chiral Nanophotonics*; Springer, 2017.



DOI: 10.1021/acsphotonics.7b00329
*ACS Photonics* 2017, 4, 1544−1551